



Coal Seam Roof: Lithology and Influence on the Enrichment of Coalbed Methane

Yunlan He^{1,2*}, Xikai Wang³, Hongjie Sun³, Zhenguo Xing³, Shan Chong¹, Dongjing Xu², Feisheng Feng³

¹State Key Laboratory of Coal Resources and Safety Mining, China University of Mining & Technology, Beijing 100083, China

²Shandong Provincial Key Laboratory of Depositional Mineralization & Sedimentary Minerals, College of Earth Science & Engineering, Shandong University of Science and Technology, Qingdao 266590, China

³College of Geoscience and Surveying Engineering, China University of Mining & Technology, Beijing 100083, China

* Corresponding author: 55069008@qq.com

ABSTRACT

To identify the lithology of coal seam roof and explore the influence of these roofs on the enrichment of coalbed methane, low-frequency rock petrophysics experiments, seismic analyses and gas-bearing trend analyses were performed. The results show that the sound wave propagation speed in rock at seismic frequencies was lower than that at ultrasound frequencies. Additionally, the P-wave velocities of gritstone, fine sandstone, argillaceous siltstone and mudstone were 1,651 m/s, 2,840 m/s, 3,191 m/s and 4,214 m/s, respectively. The surface properties of the coal seam roofs were extracted through 3D seismic wave impedance inversion. The theoretical P-wave impedance was calculated after the tested P-wave velocity was determined. By matching the theoretical P-wave impedance of the four types of rocks with that of the coal seam roofs, we identified the lithology of the roofs. By analyzing known borehole data, we found that the identified lithology was consistent with that revealed by the data. By comparing and analyzing the coal seam roof lithology and the gas-bearing trends in the study area, we discovered that the coal seam roof lithology was related to the enrichment of coalbed methane. In the study area, areas with high gas contents mainly coincided with roof zones composed of mudstone and argillaceous siltstone, and those with low gas contents were mainly associated with fine sandstone roof areas. Thus, highly compact areas of coal seam roof are favorable for the formation and preservation of coalbed methane.

Keywords: Low frequency; Rock petrophysics; Lithology; Coalbed methane; Enrichment.

Cimas con gas de filones de carbón: litología e influencia en el enriquecimiento de metano en capas de carbón

RESUMEN

Para identificar la litología de una cima con gas de filones de carbón y explorar la influencia de estas cimas en el enriquecimiento de metano en capas de carbón, se realizaron experimentos de petrofísica en rocas de baja frecuencia, análisis sísmicos y análisis de tendencias con gas. Los resultados muestran que la velocidad de propagación de la onda de sonido en roca a frecuencias sísmicas fue menor que la de las frecuencias de ultrasonido. Además, las velocidades de la onda P de arenisca, arenisca fina, limolita arcillosa y lutita fueron 1.651 m/s, 2.840 m/s, 3.191 m/s y 4.214 m/s, respectivamente. Las propiedades de la superficie de los techos con gas de filones de carbón se extrajeron mediante inversión de impedancia de onda sísmica 3D. La impedancia teórica de la onda P se calculó después de determinar la velocidad de la onda P probada. Al hacer coincidir la impedancia teórica de la onda P de los cuatro tipos de rocas con la de las cimas con gas de filones de carbón, se identificó la litología de las cimas. Al analizar los datos conocidos del pozo, se encontró que la litología identificada era consistente con la revelada por los datos. Al comparar y analizar la litología de la cima con gas de filones de carbón y las tendencias con gas en el área de estudio, descubrimos que la litología de esta cima estaba relacionada con el enriquecimiento del metano de las capas de carbón. En el área de estudio, las áreas con alto contenido de gas coincidieron principalmente con zonas de techo compuestas de lutita y limolita arcillosa, y aquellas con bajo contenido de gas se asociaron principalmente con áreas de techo de arenisca fina. Por lo tanto, las áreas altamente compactas del techo con vetas de carbón son favorables para la formación y preservación del metano de las capas de carbón.

Palabras clave: baja frecuencia; petrofísica de roca; litología; carbón metano; enriquecimiento.

Record

Manuscript received: 27/04/2019

Accepted for publication: 11/07/2019

How to cite item

He, Y., Wang, X., Sun, H., Xing, Z., Chong, S., Xu, D., & Feng, F. (2019). Coal Seam Roof: Lithology and Influence on the Enrichment of Coalbed Methane. *Earth Sciences Research Journal*, 23(4), 359-364. DOI: <https://doi.org/10.15446/esrj.v23n4.84394>

Introduction

Coalbed methane exists in coal rock, and coalbed methane enrichment remains a difficult research topic. In addition to the coal seam, which influences methane enrichment (Groshon, Pashin, & McIntyre, 2009; Keđzior, 2009; Hemza, Sivek, & Jirásek, 2009; Gao et al., 2012; Moore, 2012), the coal seam roof also affects the enrichment of coalbed methane. Thus, the role of the roof has attracted increased research attention (Chen, Cui, Liu, & Lang., 2006; Zhou, 2013; Song et al., 2013). The properties of coal seam roofs are difficult to determine based on sparse borehole data; however, 3D seismic data collected at low frequencies (5-100 Hz) can greatly improve the density of control points and identification accuracy. The theories regarding the propagation velocity of sound waves in rock at seismic frequencies have not been supported by experimental data, although some have described the velocity and attenuation of sound waves in fluid-saturated rock at seismic frequencies (Ba, 2010; White, 1975; Biot, 1956). These theoretical models are mainly based on experimental data at ultrasonic frequencies (MHz). Tutuncu, Gregory, Sharma, and Podio (1998) measured the P-wave and S-wave velocities of a saline-saturated sandstone at frequencies of 10 Hz-1 MHz, and the results showed that both the P-wave and S-wave velocities displayed upward-increasing trends. Batzle, Han, and Hofmann (2006) tested and compared the propagation velocity of sound waves at seismic and ultrasonic frequencies using a low-frequency stress-strain method and an ultrasonic test. Wang, Zhao, Harris, and Quan (2012) measured the bulk modulus of different types of rocks at 600 Hz using resonance spectroscopy and compared the results with those at ultrasonic frequencies. Using a low-frequency stress-strain method, Wei, Wang, Zhao, Tang, and Deng (2015a; 2015b) discussed the factors that influence the propagation velocity of sound waves in sandstone and studied the propagation velocity of sound waves and their dispersion characteristics under different conditions. In this paper, the propagation velocity of sound waves in four types of rocks was measured and studied using a low-frequency stress-strain method. By matching the tested velocity with 3D seismic data, we identified the coal seam roof lithology to explore the influence of the roofs on the enrichment of coalbed methane. We hope that this study will improve studies of the propagation velocity of sound waves at low frequencies and the enrichment trends of coalbed methane (Hungerford, 2013; Li & Wu, 2016; Liu, 2018).

Research methods

Low-frequency rock petrophysics experiments

The samples used in the low-frequency rock petrophysics experiments included four representative types of rocks: gritstone, fine sandstone, argillaceous siltstone, and mudstone. The rocks were collected from the top of the #3 coal seam of the Permian Shanxi Formation at the Sihe Coal Mine in the southern

Qinshui Basin, China. The gritstone was coarse-grained quartz sandstone with no primary pore development, some micro-fissures, and a porosity of less than 3%. The fine sandstone was fine quartz sandstone with primary pore development and a porosity of approximately 20%. The argillaceous siltstone was composed of fine particles and miscellaneous bases with poor separation, no primary pore development, and porosity of almost 0%. The mudstone was collected from the immediate coal seam roof, was composed of argillaceous rocks, and had a porosity of 0%.

In this experiment, the physical system used to test the rock samples at low frequencies (Fig. 1) was developed by the Colorado School of Mines, and a low-frequency stress-strain method was used as the experimental method. The tested rock samples were cylindrical, with a diameter of 38 mm and a length of 50-80 mm. Each sample had cylindrical aluminum block bases and P- and S-wave probes at both ends. Additionally, longitudinal and transverse strain gauges were fixed on the aluminum block bases and rock samples, respectively.

The physical testing system can produce acoustic waves with frequencies of 3-2,000 Hz, and the vertical and transverse strains can be tested with fixed strain gauges on the aluminum block and rock samples. The Young's modulus of the aluminum block was 69.8 GPa. Each rock sample and the aluminum block bases comprised a complete unit, so their stresses were the same during the test. Notably, the stress on the aluminum block (σ_{Al}) was equal to that on the rock sample (σ_s) (Formula 1).

$$\sigma_{Al} = \sigma_s \quad (1)$$

The stress on the aluminum block (σ_{Al}) was as follows.

$$\sigma_{Al} = E_{Al} \cdot \varepsilon_{Al-v} \quad (2)$$

The Young's modulus of the rock sample (E_s) can be deduced from Formulas 1 and 2.

$$E_s = \frac{\sigma_s}{\varepsilon_{s-v}} = \frac{E_{Al} \cdot \varepsilon_{Al-v}}{\varepsilon_{s-v}} = \frac{69.8GPa \cdot \varepsilon_{Al-v}}{\varepsilon_{s-v}} \quad (3)$$

The Poisson ratio of a rock sample (ν) can be obtained by Formula 4.

$$\nu = \frac{\varepsilon_{s-v}}{\varepsilon_{s-h}} \quad (4)$$

Because the Young's modulus and Poisson ratio of a rock sample were given, the other parameters of the rock sample at different frequencies and conditions could be obtained by the formulas listed in Table 1.

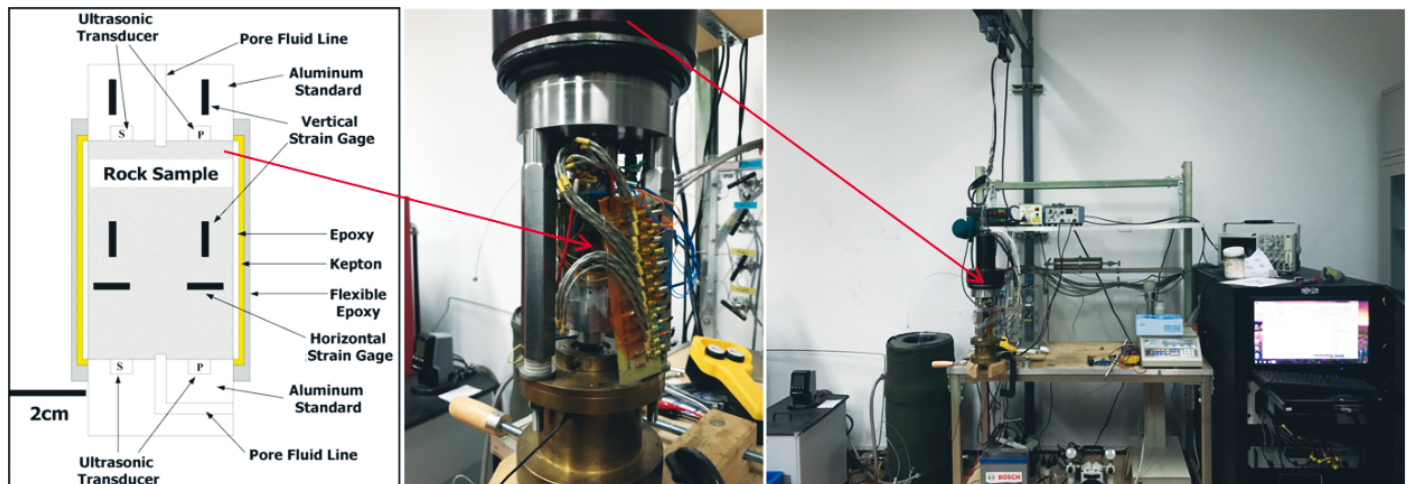


Figure 1. Physical testing system of the rock at low frequencies

Table 1. Formulas for calculating the elastic parameters of the rock samples

Elastic parameter	Formula
Shear modulus	$G = \frac{E}{2(1+\nu)}$
Bulk modulus	$K = \frac{E}{3(1-2\nu)}$
Longitudinal wave velocity	$V_p = \sqrt{\frac{K + \frac{4}{3}G}{\rho}}$
Transverse wave velocity	$V_s = \sqrt{\frac{G}{\rho}}$

3D seismic data and gas content of the study area

The 3D seismic data had a CMP mesh density of 5 m×10 m, with 16 stacked layers. First, the data underwent a series of processes, including static correction, amplitude preservation, denoising, deconvolution, and velocity analysis. Then, post-stack wave impedance inversion was performed using the processed data. In terms of the stratum of the coal seam roof, the depth of the coal seam roof can be determined by observing the strong reflection interface formed by the coal seam and the surrounding rock. From the post-stack wave impedance inversion data, the P-wave impedance surface properties of the coal seam roof strata were extracted. To identify the coal seam roof lithology, the properties of the coal seam roof were correlated and matched with the product of the propagation velocity of the sound waves and the density of rock measured in the low-frequency experiments.

Using the gas contents measured in boreholes, the content difference and distribution were analyzed. The study area was 3.57 km long and 0.87 km wide, with an area of approximately 3.10 km². The gas contents were collected from 20 wells, and measurements were obtained from cores via a direct analytic method for the #3 coal seam. When analyzing the gas content, a content distribution map was drawn using the Kriging interpolation method according to the gas contents of the boreholes.

Results

Results of the low-frequency experiments

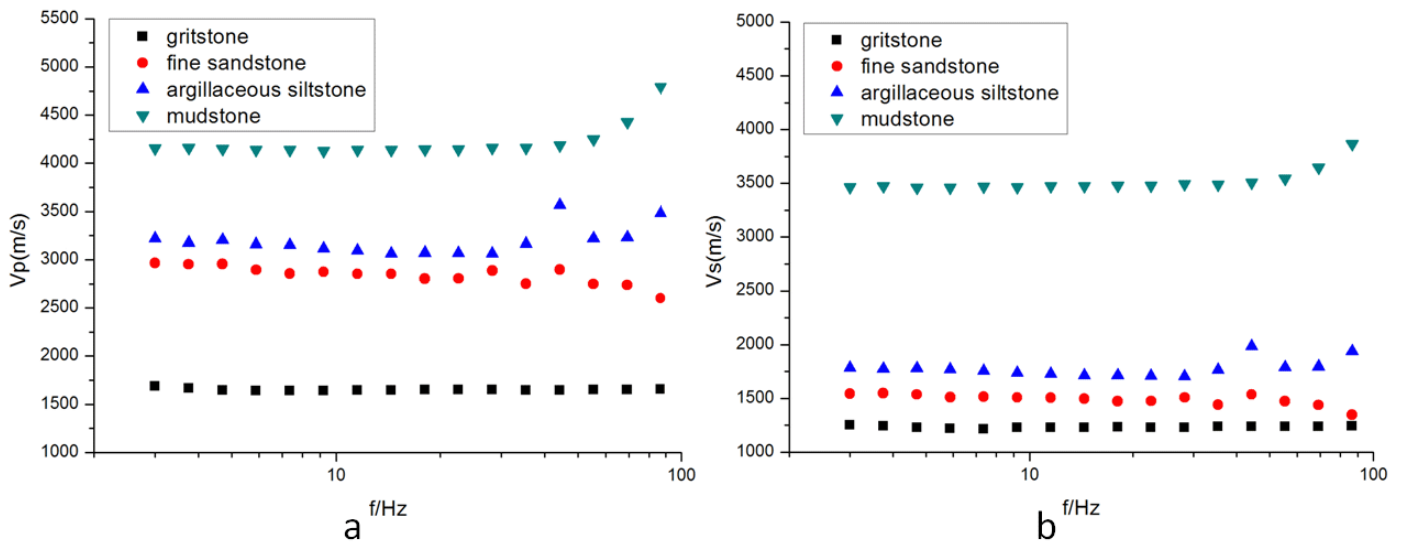
The propagation velocity of sound waves in the four types of rocks was measured at 16 frequencies from 3-100 Hz. The P-wave and S-wave velocities of the rocks at the 16 frequencies are shown in Fig. 2. Fig. 2a shows the relationship between the P-wave velocity and frequency. The P-wave velocity of the gritstone varies little at different frequencies, with an average of 1,651 m/s. The P-wave velocities of the fine sandstone, argillaceous siltstone and mudstone exhibited little variability, with average values of 2,840 m/s, 3,191 m/s and 4,214 m/s, respectively. Fig. 2b shows the relationship between the S-wave velocity and frequency, and the resulting trends are similar to those for the P-wave velocity, but with smaller variations and average values of 1,233 m/s, 1,492 m/s, 1,778 m/s and 3,514 m/s for the four materials. By comparing the propagation velocity of sound waves in the four types of rocks, we found that both the P-wave and S-wave velocities successively increased at different frequencies.

Wave impedance properties of the coal seam roof

Because wave impedance inversion is important for identifying rock properties, it is a common method used to identify sandstone and mudstone based on the sound wave velocity and density log curves. Figure 3 shows the P-wave impedance surface properties of the #3 coal seam roof in the study area. The depth of the roof was 10 m higher than the bottom boundary of the #3 coal seam, and the P-wave impedance varies between the roof and the boundary. According to the characteristics of the P-wave impedance of the roof, the impedance was divided into three types: yellow-red P-wave impedance (6,400 m/s·g/cc to 7,800 m/s·g/cc), blue P-wave impedance (7,800 m/s·g/cc-9,400 m/s·g/cc) and purple P-wave impedance (> 9,400 m/s·g/cc). The P-wave impedance, with a range of approximately 6,400 m/s·g/cc-10,000 m/s·g/cc, greatly differed and displayed obvious partitioning and zoning.

Gas content of the study area

The gas properties in the study area were analyzed with a Kriging interpolation method based on the gas contents of the boreholes in the #3 coal seam (Fig. 4). The overall gas content in the area was high but considerably

**Figure 2.** Relationships between the propagation velocity of sound waves in the four types of rocks and the frequency

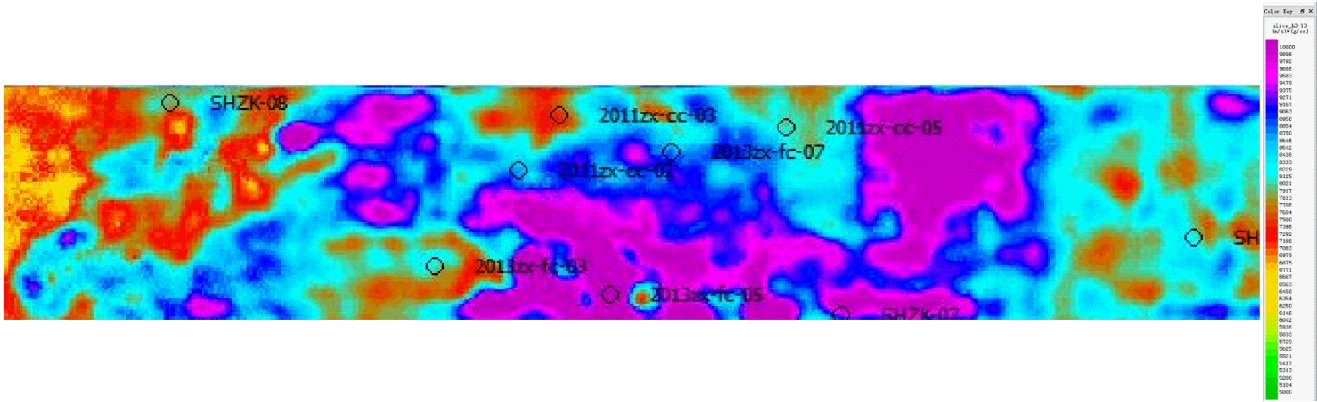


Figure 3. P-wave impedance properties of the #3 coal seam roof

varied. The study area (3.10 km²) exhibited a gas content ranging from approximately 19 m³/t to nearly 29 m³/t, a difference of nearly 10 m³/t. Three sub-areas with gas contents greater than 27 m³/t were observed and are colored in red in Figure 5. Four sub-areas with gas contents lower than 20 m³/t were observed and are colored in yellow in Figure 5.

Discussion

Wave impedance inversion can be used to analyze the properties of coal seam roof strata. Wave impedance is the product of the propagation velocity of a sound wave in rock and the density of the rock, and it can be used to identify the lithology. However, sandstone and mudstone cannot be distinguished simply by wave impedance and can be influenced by many factors. Moreover, the logging velocity was obtained at high frequencies in the process of wave impedance inversion. After well logging calibration was performed for the velocity and density log curves and 3D seismic data, wave impedance inversion was performed for data interpolation.

Low-frequency experiments were performed to obtain the propagation velocity of sound waves in four types of rock, and the velocity was used to calculate the theoretical wave impedance. The results did not match the wave impedance values obtained by 3D seismic inversion at higher frequencies. For example, Murphy (1984) measured the propagation velocity of sound waves in sandstone at different frequencies using the resonance bar technique, and the

results showed that the propagation velocity of sound waves in sandstone at 500 kHz was 10-25% higher than that at 5 kHz. Tutuncu et al. (1998) measured the propagation velocity of sound waves in saline-saturated sandstone, and the P-wave velocity and S-wave velocity increased by 33% and 20%, respectively, as the frequency increased from 10 Hz to 1 MHz. Batzle et al. (2006) measured the P-wave velocity of high porosity and high permeability sandstone (with a porosity of 35% and a permeability of 8.7×10⁻¹² m²) using a stress-strain method and ultrasonic measurement technique. The P-wave velocity of the 90% saturated sandstone at 0.8 MHz was 32% higher than that at 5-10 Hz (Batzle et al., 2006). These experiments confirmed that the propagation velocity of sound waves at seismic frequencies is lower than that at ultrasonic frequencies.

According to the collected borehole data, the coal seam roof was mainly composed of gritstone, medium sandstone, fine sandstone, sandy mudstone, siltstone, and mudstone. In this study, the propagation velocity of sound waves was monitored at both low and ultrasonic frequencies (1 MHz). The P-wave velocity at low frequencies was lower than that at ultrasonic frequencies, but the P-wave velocities of rocks with different lithologies considerably differed. To better match the theoretical wave impedance calculated according to the experimental results, the P-wave velocity was increased by 20% to compensate for the difference in velocity due to the difference in frequency. The specific data are shown in Table 2.

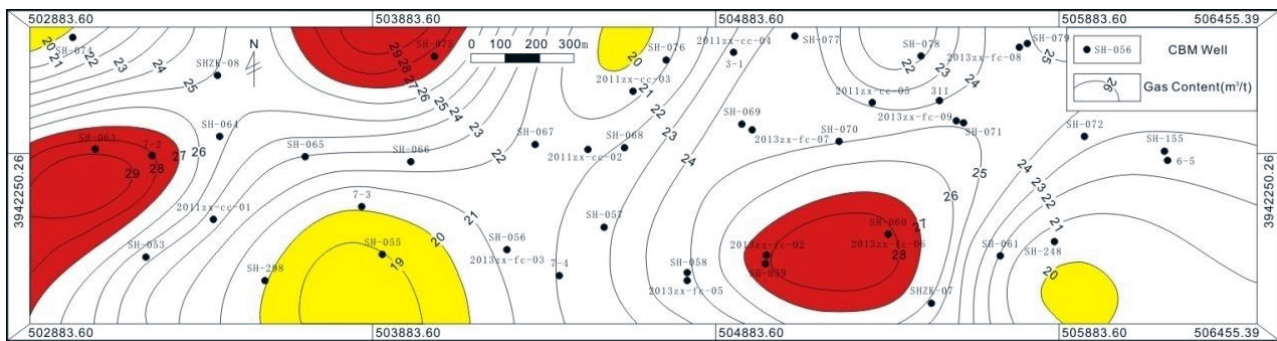


Figure 4. Gas content distribution in the study area

Table 2. The P-wave velocity and P-wave impedance of the rocks

Lithology	Density (g/cm ³)	V _{p-Lf} (m/s)	V _{p-1MHz} (m/s)	V _{p-Lf} × (1+20%) (m/s)	V _{p-Lf} × Density (m/s·g/cc)	(1.2 × V _{p-Lf}) × Density (m/s·g/cc)
Gritstone	2.30	1651	1805	1981	3797	4557
Fine sandstone	1.95	2840	3854	3408	5538	6646
Argillaceous siltstone	2.41	3191	3588	3829	7690	9228
Mudstone	2.20	4214	5070	5057	9270	11125

*V_{p-Lf} is the V_p value of the low-frequency condition, and V_{p-1MHz} is the V_p value of the 1 MHz frequency condition.

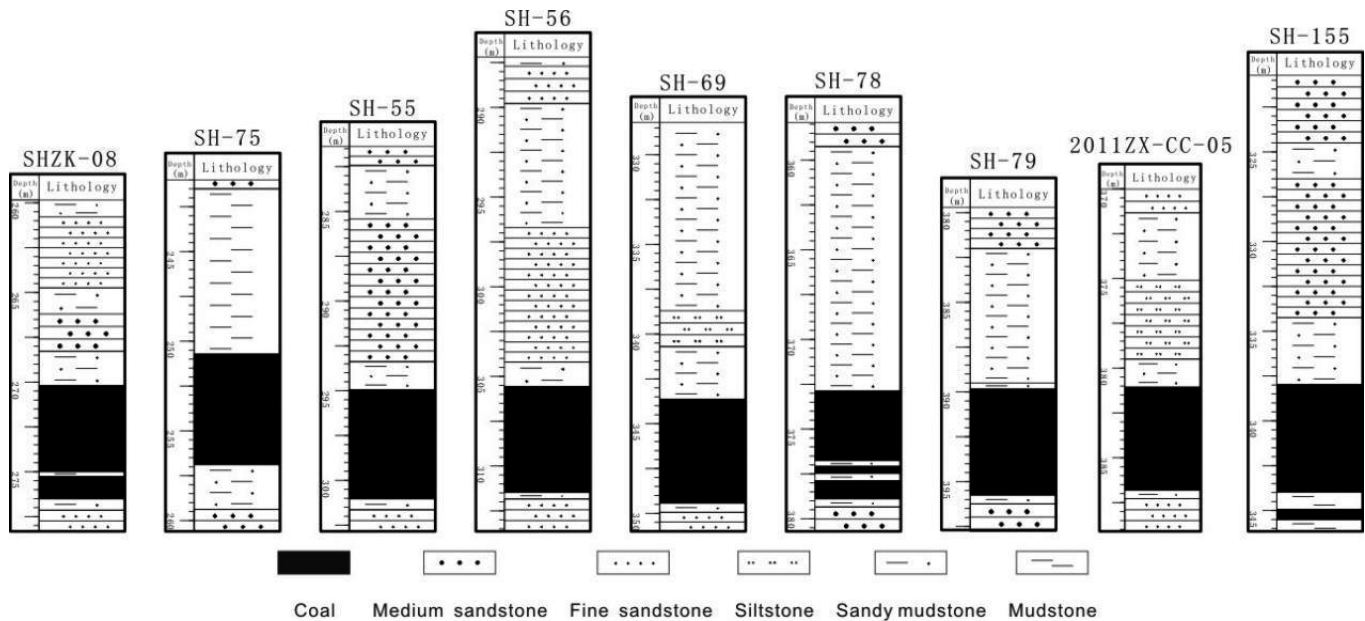


Figure 5. The lithological column sections from the known wells

The difference in wave impedance for different lithologies was essential for matching the theoretical wave impedance with the wave impedance of 3D seismic inversion. The P-wave velocity of the gritstone was low, possibly due to the existence of micro-fissures. The P-wave impedance did not match that based on 3D seismic inversion, and the weighted P-wave impedance of the gritstone was 4,557 m/s·g/cc. The P-wave impedance of fine sandstone was 6,646 m/s·g/cc, which fell within the scope of the yellow-red wave impedance (6,400 m/s·g/cc–7,800 m/s·g/cc) when matching the wave impedance obtained by 3D seismic inversion. The P-wave impedance of argillaceous siltstone was 9,228 m/s·g/cc, which is within the scope of blue wave impedance (7,800 m/s·g/cc–9,400 m/s·g/cc). Additionally, the P-wave impedance of the mudstone exceeded 10,000 m/s·g/cc, which is within the scope of purple P-wave impedance (> 9,400 m/s·g/cc).

The lithology of the identified coal seam roof was tested according to the known borehole data. The depth of the coal seam roof was 10 m higher than the bottom boundary of the coal seam, and 2000 m/s was selected as the average propagation velocity of the sound wave. Fig. 5 shows the coal seam of the selected test well and the top and bottom lithology. The identified coal seam roof lithology was consistent with that revealed by the borehole data. In terms of lithological identification, sandstone could not be distinguished from fine sandstone, and sandy mudstone could not be distinguished from mudstone. However, the fine sandstone, siltstone and mudstone could be distinguished.

In addition to coal seams, coal seam roof also influence the enrichment of coalbed methane. During the diagenetic evolution of coal, a ton of coal, from lignite to anthracite, can produce 268–393 m³ of gas (Zhang & Li, 1988), but only a fraction of this coalbed methane is eventually preserved. The coal seam roof directly contacts the coal seam and undergoes diagenetic evolution together with the coal seam, and the compactness of the coal seam roof has a direct influence on the residual coalbed methane content (Li et al., 2003; Liu, Li, Yang, Liu, & Yan, 2012). By comparing and analyzing the coal seam roof lithology and gas content, we found that the coal seam roof lithology is related to the enrichment of coalbed methane. The coal seam roof in the three areas with high gas contents was mainly mudstone and argillaceous siltstone, and the coal seam roof in the four areas with low gas contents was mainly fine sandstone. The mudstone and argillaceous siltstone, which are highly compact, were more conducive to the preservation of coalbed methane, and the fine sandstone, which is poorly compact, was not.

Conclusion

In this paper, the variable propagation velocity of sound waves in four types of rock was measured at 3–100 Hz using a low-frequency stress-strain method. The P-wave and S-wave velocities of the gritstone, fine sandstone,

argillaceous siltstone, and mudstone successively increased at the same frequency. The propagation velocity of sound waves in the four types of rock at seismic frequencies was lower than that at higher frequencies. After the P-wave velocities obtained via testing were considered, the theoretical P-wave impedance of the four types of rocks was calculated, and the values were then matched with the wave impedance values of seismic inversion for the coal seam roof. The roof was mainly composed of mudstone, argillaceous siltstone, and fine sandstone, and the boreholes verified that the lithology. The lithology of the roof is related to the enrichment of coalbed methane. The roof in areas with high gas contents was mainly mudstone and argillaceous siltstone, and that in areas with low gas contents was mainly fine sandstone. Compact areas of the coal seam roof were more conducive to the formation and preservation of coalbed methane.

Acknowledgments

The project was financially supported by the subject of Open Fund of State Key Laboratory of Coal Resources and Safe Mining, China University of Mining & Technology, Beijing (SKLCSRSM19ZZ01), the Fundamental Research Funds for the Central Universities (2019QMO1) and the National Natural Science Foundation of China (41602168).

References

- Ba, J. (2010). Wave propagation theory in double-porosity medium and experimental analysis on seismic responses. *Scientia Sinica (Physica, Mechanica & Astronomica)*, 40(11), 1398–1409.
- Batzle, M. L., Han, D. H., & Hofmann, R. (2006). Fluid mobility and frequency-dependent seismic velocity—Direct measurements. *Geophysics*, 71(1), N1–N9.
- Biot, M. A. (1956). Theory of propagation of elastic waves in a fluid-saturated porous solid. I. Low-frequency range. *The Journal of the Acoustical Society of America*, 28(2), 168–178.
- Chen, T. J., Cui, R. F., Liu, E. R., & Lang, Y. Q. (2006). Prediction of coal seam methane enriched areas using seismic data. *Journal of China University of Mining & Technology (English Edition)*, 16(4), 421–424.
- Gao, L. J., Tang, D. Z., Xu, H., Meng, S. Z., Zhang, W. Z., Meng, Y. J., & Wang, J. J. (2012). Geologically controlling factors on coal bed methane (CBM) productivity in Liulin. *Journal of Coal Science and Engineering (China)*, 18(4), 362–367.

- Groshong Jr, R. H., Pashin, J. C., & McIntyre, M. R. (2009). Structural controls on fractured coal reservoirs in the southern Appalachian BLACK Warrior foreland basin. *Journal of Structural Geology*, 31, 874-886.
- Hemza, P., Sivek, M., & Jirásek, J. (2009). Factors influencing the methane content of coal beds of the Czech part of the Upper Silesian Coal Basin, Czech Republic. *International Journal of Coal Geology*, 79, 29-39.
- Hungerford, F. (2013). In-seam directional drilling for improving safety and productivity in underground coal mines. *Journal of Mines, Metals and Fuels*, 61(7-8), 213-218.
- Kędzior, S. (2009). Accumulation of coal-bed methane in the south-west part of the Upper Silesian Coal Basin (southern Poland). *International Journal of Coal Geology*, 80, 20-34.
- Li, T., & Wu, C. (2016). Influence of pressure, coal structure and permeability on CBM well productivity at various burial depths in South Yanchuan Block, China. *Earth Sciences Research Journal*, 20(3), D1-D9. DOI: <https://doi.org/10.15446/esrj.v20n3.58000>
- Li, W. Z., Wang, Y. B., Cui, S. H., Xian, B. A., Chen, C. H., & Wang, X. H. (2003). Analysis of the generation conditions of coalbed gas reservoir, Southern Qinshui Basin. *Coal Geology & Exploration*, 31(2), 23-26.
- Liu, Y. H., Li, M. X., Yang, X., Liu, C. C., & Yan, L. (2012). Laws of coalbed methane enrichment and high productivity in the Fanzhuang Block of the Qinshui Basin and development practices. *Natural Gas Industry*, 32(4), 29-32.
- Liu, Z. (2018). Economic analysis of methanol production from coal/biomass upgrading. *Energy Sources Part B-Economics Planning and Policy*, 13(1), 66-71.
- Moore, T. A. (2012). Coalbed methane: A review. *International Journal of Coal Geology*, 101, 36-81.
- Murphy, W. F. β. (1984). Acoustic measures of partial gas saturation in tight sandstones. *Journal of Geophysical Research*, 89(B13), 11549-11559.
- Song, Y., Liu, S. B., Ju, Y. W., Hong, F., Jiang, L., Ma, X. Z., & Wei, M. M. (2013). Coupling between Gas Content and Permeability controlling Enrichment Zones of high Abundance Coal Bed Methane. *Acta Petrolei Sinica*, 34(3), 417-426.
- Tutuncu, A. N., Gregory, A. R., Sharma, M. M., & Podio, A. L. (1998). Nonlinear viscoelastic behavior of sedimentary rocks, Part I: Effect of frequency and strain amplitude. *Geophysics*, 63(1), 184-194.
- Wang, S. X., Zhao, J. G., Harris, J. M., & Quan, Y. (2012). Differential acoustic resonance spectroscopy for the acoustic measurement of small and irregular samples in the low frequency range. *Journal of Geophysical Research Atmospheres*, 117(B6), 6203.
- Wei, X., Wang, S. X., Zhao, J. G., & Deng, J. X. (2015a). Laboratory investigation of influence factors on Vp and Vs in tight sandstone. *Geophysical Prospecting for Petroleum*, 54(1), 9-16.
- Wei, X., Wang, S. X., Zhao, J. G., Tang, G. Y., & Deng, J. X. (2015b). Laboratory study of velocity of the seismic wave in fluid-saturated sandstones. *Chinese Journal of Geophysics*, 58(9), 330-338.
- White, J. E. (1975). Computed seismic speeds and attenuation in rocks with partial gas saturation. *Geophysics*, 40(2), 224-232.
- Zhang, W & Li, X. (1988). Analysis of the hydrocarbon-producing potential of main coal measures source rocks in China. *Coal Geology & Exploration*, 16(3), 31-37.
- Zhou, Q. Q. (2013). Geological control law of coalbed methane accumulation of heshun block in Qinshui Basin. *China Coalbed Methane*, 10(2), 12-15.